Analysis and Design of Robust Motion Controllers in the Unified Framework

Bong Keun Kim
Graduate Student, Department of Mechanical Engineering, Pohang University of Science and Technology, San 31, Hyoja-Dong, Nam-Gu, Pohang, 790-784, Korea
e-mail: kbk@postech.ac.kr

Hyun-Taek Choi
Graduate Student, School of Electrical Engineering and Computer Science, Hanyang University, 1271, Sa 1-Dong, Ansan, 425-791, Korea
e-mail: finding@hanmir.com

Wan Kyun Chung
Professor, Department of Mechanical Engineering, Pohang University of Science and Technology, San 31, Hyoja-Dong, Nam-Gu, Pohang, 790-784, Korea
e-mail: wkchung@postech.ac.kr

Il Hong Suh
Professor, School of Electrical Engineering and Computer Science, Hanyang University, 1271, Sa 1-Dong, Ansan, 425-791, Korea
e-mail: ihsuh@email.hanyang.ac.kr

Model based disturbance compensating methods such as disturbance observer, robust control with adaptive algorithm, enhanced internal model control are well known control structures for robust motion controller which can satisfy desired performance and robustness of high-speed/high-accuracy positioning systems. In this paper, these are analyzed in the unified framework and their design method is proposed. To do this, a generalized disturbance attenuation framework named RIC (robust internal-loop compensator) structure is introduced. Through parameterization based on RIC, it is shown that there are inherent equivalences in their structures and the proposed RIC gives a general design framework for the model based disturbance compensating methods. Through simulation, the proposed method is verified.
[DOI: 10.1115/1.1468995]

Keywords: Two-Loop Structure, Robust Internal-Loop Compensator, Disturbance Observer, Unified Framework

1 Introduction

With the growing interests on high performance of a mechanical positioning system, more accurate and robust control algorithms are required. However, the dynamic equation of complex mechanical system is highly nonlinear and strongly coupled. Moreover, since system parameters and external disturbances cannot be exactly measured, it becomes more difficult to meet higher performance specifications. A variety of advanced controller design methods have been proposed to overcome these difficulties. Disturbance observer (DOB) [1–9], robust control with adaptive algorithm (RCA) [10–12], model based disturbance attenuation (MBDA) [12], and enhanced internal model control (IMC) [13] are good examples. These methods commonly require the design of two-loop structures. One is the design of internal-loop compensator for robustness, the other is the design of the external-loop controller for desired performance specifications. In such schemes, the internal-loop compensator generates corrective control inputs to reject disturbance as much as possible to force the actual system to become a given nominal model. Thus, the actual plant with such an internal-loop compensator can be regarded as a nominal model if the internal-loop compensator works well. On the other hand, the external-loop controller is designed to enhance overall system performance, where the controller design is carried out for the nominal model.

DOB based controller design is one of the most popular methods in the field of motion control. It has been widely used in industrial applications because of its simple structure and robust properties. Using an inverse of a nominal model and a low-pass filter, DOB estimates the disturbance and the estimate is utilized as a cancellation signal. Thus, DOB can make the dynamics between external control input to the plant output robust in the presence of uncertainties and disturbances. RCA was proposed to improve the performance of DOB, which has advantages of both adaptive control and robust control based on sliding mode concept. Hence this can handle large parameter variations and has a flexible structure to further improvement of transient response and tracking performance. As one of model based robust control method, MBDA was proposed and compared with DOB and RCA. But, the comparison was not carried out systematically, and there are no explanations on structural relationship among these three types of structures. Based on the conventional structure of IMC, a modified scheme for the uncertainty reduction and robustness enhancement of IMC system was also proposed. It was shown that the robustness of IMC systems can be further improved with proper structure modification while retaining the inherent advantages of the IMC structure.

Unfortunately, however, the above robust motion controllers with two-loop structure have not been compared by structural relationship. This is partially due to the difficulty in making a unified controller structure to incorporate these controllers. This is the motivation of this paper. The purpose of this paper is to design a robust motion controller for high-speed/high-accuracy positioning systems in a unified framework, as well as a qualitative/quantitative comparison with conventional disturbance compensating methods. To do this, a framework named RIC (robust internal-loop compensator) is proposed. Since RIC has a very general structure which can include these methods analytically, robust controllers with two-loop can be analyzed in the RIC framework and structural relationship can be addressed. Through this analysis, it is shown that there are inherent structural equivalences between RIC, DOB, RCA, and enhanced IMC.

In Section 2, a control system with two-loop structure is described and a RIC structure is proposed. In Section 3, the existing disturbance attenuation methods are analyzed in the RIC framework. In Section 4, a systematic design method for DOB is discussed. Next, in Section 5, simulation results of comparative research and design example are shown, and conclusion follows.

2 Robust Internal-Loop Compensator

2.1 Robust Control Systems With Two-Loop Structure. Model based robust control methods such as DOB, RCA, and enhanced IMC commonly require the design of two-loop structure as shown in Fig. 1 although these are designed by different criterions. The internal-loop is used as a disturbance compensator rather than a controller, so we call this *internal-loop compensator* and the external-loop is used as a controller. We call this *external-loop controller*. The actual plant with such an internal-loop compensator can be regarded as a given nominal model if the internal-loop compensator works well and the performance of whole

Contributed by the Dynamic Systems and Control Division of THE AMERICAN SOCIETY OF MECHANICAL ENGINEERS. Manuscript received by the Dynamic Systems and Control Division June 15, 2000. Associate Editor: Y. Chait.

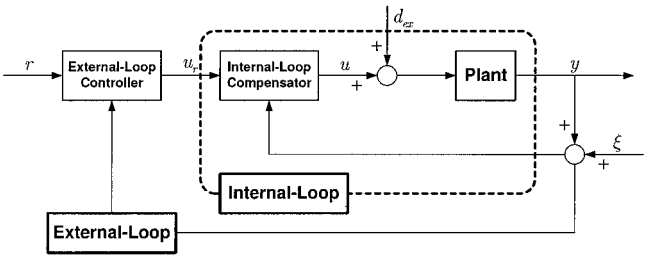

Fig. 1 Robust control system with two-loop structure

system is determined by the external controller using the nominal model. Therefore the inherent structural characteristics of model based robust control methods can be evaluated by the comparison of their internal-loop structures. Now, we propose a generalized control framework for the analysis and design of these internal-loop compensators.

2.2 Compensated Feedback System. Without loss of generality, the proposed control method is presented for systems with a single-input, single-output (SISO), which allows us to develop an intuition about the basic aspects of the proposed robust motion controller design. Figure 2 shows a compensated feedback system with prefilter $F(s)$ to achieve a specified transfer function of reference model $P_m(s)$. The plant is represented by the transfer function $P(s)$ and its output signal y. The function u_r represents a reference control input signal, y_r represents a reference model output signal, u represents a control input signal, $K(s)$ represents a feedback compensator, and d_{ex} represents an external disturbance signal and a measurement noise signal ξ is added to output y.

From the block diagram in Fig. 2, the sensitivity and complementary sensitivity functions are obtained as follows:

$$S(s)=\frac{y}{P(s)d_{ex}}=\frac{1}{1+L(s)},\quad T(s)=-\frac{y}{\xi}=\frac{L(s)}{1+L(s)} \tag{1}$$

where $L(s)=P(s)K(s)$ is the open-loop transfer function of the unity feedback system. Hence it can be easily seen that the effect of the disturbance and the measurement noise on the plant output are only determined by the plant $P(s)$ and the compensator $K(s)$. That is, the reference model $P_m(s)$ and prefilter $F(s)$ do not have an effect on the sensitivity and complementary sensitivity of Fig. 2. The transfer function from y_r to y is given by

$$T_{y_r y}(s)=F(s)\left[\frac{L(s)}{1+L(s)}\right]. \tag{2}$$

Thus, $F(s)$ is just used to make the transfer function from y_r to y be one. Therefore, the design objective is to design the compensator $K(s)$ and the prefilter $F(s)$ so that the specified robustness and performance are achieved under the parametric uncertainty and disturbance condition.

2.3 Prefilter Design. In order to design the prefilter $F(s)$, we need to reconstruct the given system to the system which has a reference model $P_m(s)$ and disturbance d. Let the plant with uncertainty be expressed as

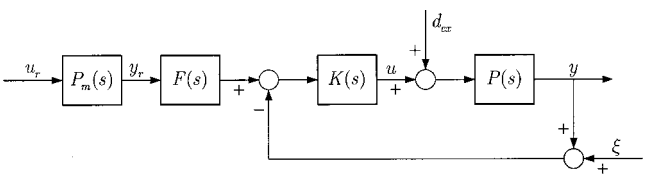

Fig. 2 Compensated unity feedback system with prefilter

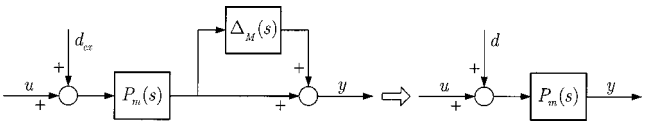

Fig. 3 Reconstruction of plant

$$P(s)=P_m(s)[1+\Delta_M(s)] \tag{3}$$

where $\Delta_M(s)$ is an allowable multiplicative uncertainty. Then, the plant can be reconstructed as shown in Fig. 3. From the input-output equivalence of Fig. 3, d is given by

$$d=\left[\frac{P(s)}{P_m(s)}-1\right]u+\left[\frac{P(s)}{P_m(s)}\right]d_{ex}. \tag{4}$$

Equation (4) with Eq. (3) is formulated as

$$d=\Delta_M(s)u+[1+\Delta_M(s)]d_{ex}, \tag{5}$$

which satisfies an important structural property called as *matching condition*, namely, it enters the state equation exactly at the point where the control variable enters. Based on Fig. 2 and Eq. (2), one of the best candidates for $F(s)$ can be chosen as follows:

$$F(s)=\left[\frac{L_m(s)}{1+L_m(s)}\right]^{-1}=\frac{1}{G_{L_m}(s)} \tag{6}$$

where $L_m(s)=P_m(s)K(s)$ and $G_{L_m}(s)$ is the transfer function of a reference closed-loop system with the reference model $P_m(s)$ and compensator $K(s)$, which is shown in Fig. 4. Thus $|T_{y_r y}(j\omega)|\approx 1$ can be achieved. Prefilter $F(s)$, in a crude way, approximates PD type transfer function. Therefore this enhances transient performance and leads the phase of the unity feedback system in Fig. 2.

Alternatively, Fig. 2 with Eq. (6) can be equivalently transformed into Fig. 5 [14]. In this figure, the difference between reference model output and measured plant output is defined as model following error:

$$e_r=y_r-(y+\xi). \tag{7}$$

Then, the control input has the form of

$$u=u_r+K(s)e_r+u^*, \tag{8}$$

where u^* is an optional control input to compensate nonlinear disturbances [15]. Note that the second term on the right-hand side in Eq. (8) can be interpreted as a control input based on Lyapunov redesign [16,17]. In this paper, the structure in Fig. 5 with the control input Eq. (8) is defined as robust internal-loop compensator(RIC) [18,19].

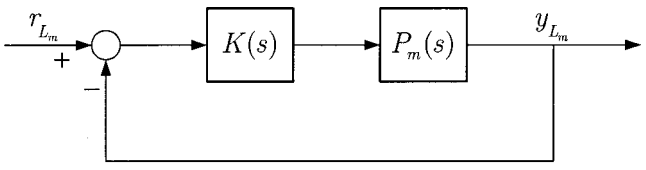

Fig. 4 Reference closed-loop system

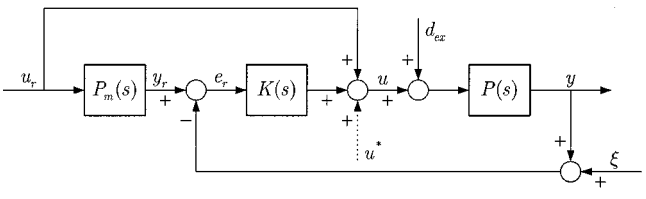

Fig. 5 Robust internal-loop compensator structure

From the block diagram in Fig. 5, the plant output y can be expressed in terms of the reference control input u_r, external disturbance d_{ex}, and measurement noise ξ:

$$y=\left[P_m(s)\left(1+\frac{\Delta_M(s)}{1+L(s)}\right)\right]u_r+\left[\frac{P(s)}{1+L(s)}\right]d_{ex}-\left[\frac{L(s)}{1+L(s)}\right]\xi. \tag{9}$$

As a result, the sensitivity and complementary sensitivity in Eq. (1) are obtained as before. Therefore, if $K(s)$ is designed in optimal sense, the specified robustness and performance can be achieved for the system in the presence of uncertainties and disturbances. And also this makes the actual plant behave like a reference model $P_m(s)$.

3 Unified Analysis of Disturbance Compensation Methods

3.1 DOB in the RIC Framework. It is well known that disturbance observer(DOB) makes a system robust using Q-filter which cuts off the disturbance in low frequency region. Figure 6 shows the structure of DOB. From the block diagram in Fig. 6, the input-output relationship can be expressed as

$$y=\left[\frac{P(s)P_n(s)}{\chi(s)}\right]u_r+\left[\frac{P(s)P_n(s)\{1-Q(s)\}}{\chi(s)}\right]d_{ex}-\left[\frac{P(s)Q(s)}{\chi(s)}\right]\xi, \tag{10}$$

where $\chi(s)=P_n(s)+[P(s)-P_n(s)]Q(s)$. Below the cutoff frequency of $Q(s)$, $|Q(j\omega)|\approx 1$ is achieved. Hence low frequency disturbances are attenuated and mismatch between plant and nominal model is compensated in the low frequency region. Thus the behavior of real plant is to be the same as given nominal model. On the other hand, above the cutoff frequency of $Q(s)$, $|Q(j\omega)|\approx 0$ is achieved. Hence high frequency measurement noise is attenuated. Therefore, in the design of a DOB, the most important design parameter is the low-pass filter Q, and the main concern is the tradeoff between making $|Q(j\omega)|$ small and $|1-Q(j\omega)|$ small.

Ohnishi used a first-order filter for Q [20]. Umeno and Hori refined the DOB based on the 2-DOF controller and suggested Q-filter which has the form of

$$Q(s)=\left[1+\sum_{k=1}^{N-r}a_k(\tau s)^k\right]\left[1+\sum_{k=1}^{N}a_k(\tau s)^k\right]^{-1} \tag{11}$$

where N is the order of $Q(s)$, τ is a filter time constant, and r is the relative degree of $Q(s)$ [21]. Yamada et al. proposed a high order DOB which can achieve rapid response and lower sensitivity to the disturbance by virtue of higher order integral element [22]. But, they also showed that the high order DOB causes less damping characteristics because of large phase lag.

In this paper, unlike the typical design method of Q-filter, we propose a systematic Q-filter design method in the proposed RIC framework. First, let us analyze DOB in the proposed RIC framework. The reference model and the prefilter of RIC are chosen as follows:

$$P_m(s)=P_n(s),\quad F(s)=\left[\frac{L_n(s)}{1+L_n(s)}\right]^{-1}=\frac{1}{Q(s)}, \tag{12}$$

where $P_n(s)$ is a proper function without RHP poles and $L_n(s)=P_n(s)K(s)$. Thus, $Q(s)$ is given by the transfer function of the nominal closed-loop system. After recalculating this equation for $K(s)$, if $K(s)$ is substituted into Fig. 5, then an equivalent structure in Fig. 7 is obtained and this can be transformed equivalently to a structure of DOB in Fig. 6. This means that if a compensator $K(s)$ is designed for the nominal model $P_n(s)$ in order to satisfy a given performance and robustness criterion, optimal Q-filter of DOB is systematically designed which has the optimality under the given specific conditions, because the transfer function of the unity feedback system with $P_n(s)$ and $K(s)$ is $Q(s)$. And also the disturbance attenuation characteristics of the designed closed-loop system can be easily analyzed based on $Q(s)$.

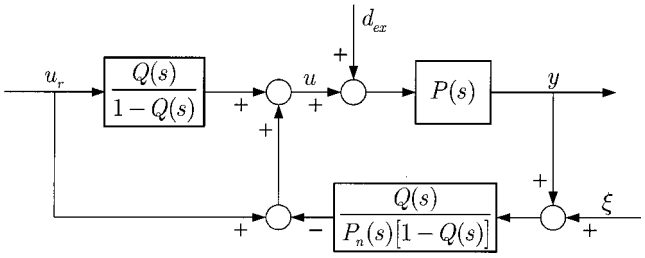

Fig. 7 Equivalent structure of RIC using $P_n(s)$ and $Q(s)$

3.2 RCA in the RIC Framework. In order to enhance the performance of DOB, robust control with adaptive algorithm-(RCA) was proposed by Yao et al. [10]. Figure 8 illustrates the structure of RCA for a high-accuracy positioning system [11,12]. The equation of motion for this system can be expressed as

$$J\ddot{y}+B\dot{y}+F_r(\dot{y})-d_{ex}=u \tag{13}$$

where J is the inertia, B is the damping coefficient, u is the control input, y is the output of interest, $F_r(\dot{y})$ is the friction term including stiction and Coulomb friction, and d_{ex} is the uncertain external disturbance whose magnitude is bounded as $d_{ex}\in[d_m,d_M]$ where d_m and d_M are known constants. The objective of the control is to synthesize a control input u such that the resulting system from reference command μ to plant output y behaves like its nominal model, even under the presence of the nonlinear friction $F_r(\dot{y})$ and external disturbance d_{ex}. Therefore, ideal reference command is expressed as

$$J_n\ddot{y}+B_n\dot{y}=\mu \tag{14}$$

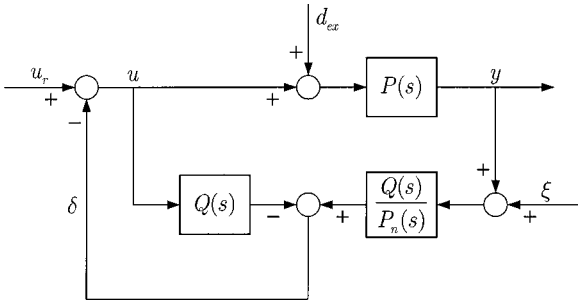

Fig. 6 Disturbance observer

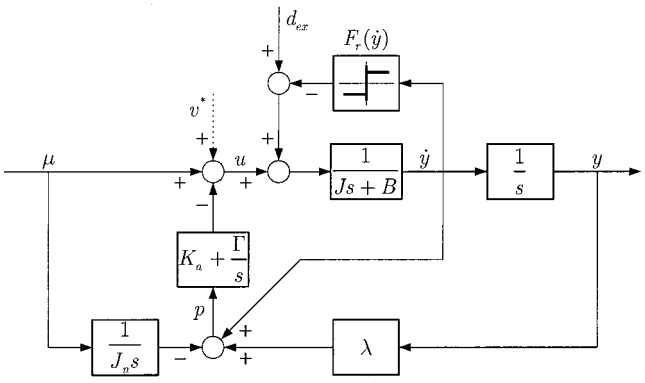

Fig. 8 Robust control with adaptive algorithm

where J_n and B_n are the nominal value of J and B, respectively. A switching-function-like quantity p is defined as

$$p=\dot{y}+\lambda y-\frac{1}{J_n}\int_0^t \mu(\tau)d\tau \tag{15}$$

where $\lambda=B_n/J_n$. Hence RCA has a form of

$$u=\mu+\widehat{F_r}(\dot{y})-\widehat{d_{ex}}-K_a p \tag{16}$$

where $K_a>0$, $\widehat{F_r}(\dot{y})$ is any fixed friction compensation, and $\widehat{d_{ex}}$ is the estimate of the external uncompensated disturbance. If $\widehat{F_r}(\dot{y})-\widehat{d_{ex}}$ is defined as an additional estimation term u^*, then the RCA can be expressed as

$$u=\mu-K_a p+u^*. \tag{17}$$

Note here that μ is an arbitrary reference control input. In Eq. (14), it is assumed that the output of nominal model is identical with plant output y if μ is applied to given nominal model. That is,

$$y=\left(\frac{1}{J_n s^2+B_n s}\right)\mu. \tag{18}$$

However, since Eq. (14) or (18) is an ideal equation under the assumption of no modeling uncertainties, we define the output of nominal model as a new variable y_r in order to distinguish between the ideal and real situations. Hence

$$y_r=\left(\frac{1}{J_n s^2+B_n s}\right)\mu \quad \text{or} \quad J_n\ddot{y}_r+B_n\dot{y}_r=\mu \tag{19}$$

and then the switching-function-like quantity p can be arranged as

$$p=-\dot{e}_r-\lambda e_r \tag{20}$$

where $e_r=y_r-y$, which was defined in Eq. (7).

Now, we can derive the parameters of RIC from Eq. (17), (19), and (20). The nominal model and the compensator are obtained from the above equations as follows:

$$P_n(s)=\frac{1}{J_n s^2+B_n s}, \quad K(s)=K_a(s+\lambda). \tag{21}$$

Therefore, $Q(s)$ is obtained from Eq. (12):

$$Q(s)=\frac{g}{s+g} \tag{22}$$

where $g=K_a/J_n$ is the cutoff frequency.

In order to further improve the performance, the following adaptation rule was introduced:

$$\dot{\widehat{d_{ex}}}=\begin{cases}0, & \text{if } \begin{cases}\widehat{d_{ex}}=d_M & \text{and } p>0\\ \widehat{d_{ex}}=d_m & \text{and } p<0\end{cases}\\ \Gamma p, & \text{otherwise}\end{cases} \tag{23}$$

where Γ is the adaptation rate. If we assume $d_m<\widehat{d_{ex}}(t)<d_M$ for all t, then the RCA in Fig. 8 can be expressed as

$$u=\mu-K_a p-\Gamma\int_0^t p(\tau)d\tau+v^* \tag{24}$$

where v^* is $\widehat{F_r}(\dot{y})$. Therefore, the nominal model and the compensator can be calculated as

$$P_n(s)=\frac{1}{J_n s^2+B_n s}, \quad K(s)=\left(K_a+\frac{\Gamma}{s}\right)(s+\lambda), \tag{25}$$

and $Q(s)$ is obtained as following equation whose order is two:

$$Q(s)=\frac{K_a s+\Gamma}{J_n s^2+K_a s+\Gamma}. \tag{26}$$

Although $P_n(s)$ and $K(s)$ can be chosen as

$$P_n(s)=\frac{1}{J_n s}, \quad K(s)=K_a+\frac{\Gamma}{s}, \tag{27}$$

it can be easily seen that the resulting $Q(s)$ is the same as Eq. (26). This interpretation is possible because the controllers are systematically analyzed based on structural characteristics of the proposed RIC.

Figure 9 illustrates the equivalent structures of RCA, which is the same as RIC in the structural view. Actually, if $Q(s)$ is chosen

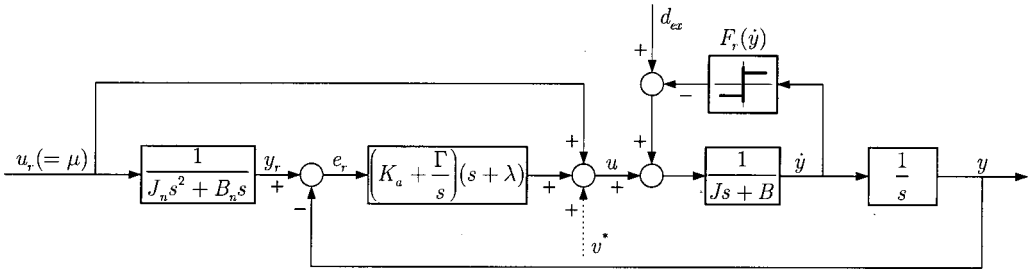

(*a*) Representation of RCA using (25)

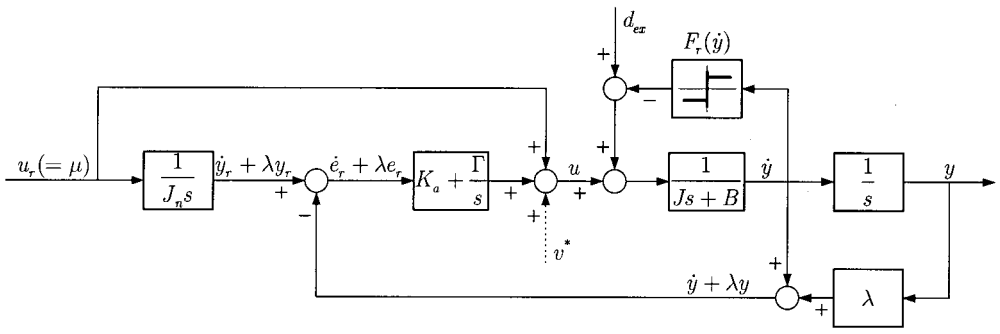

(*b*) Representation of RCA using (27)

Fig. 9 Equivalent representations of RCA structure

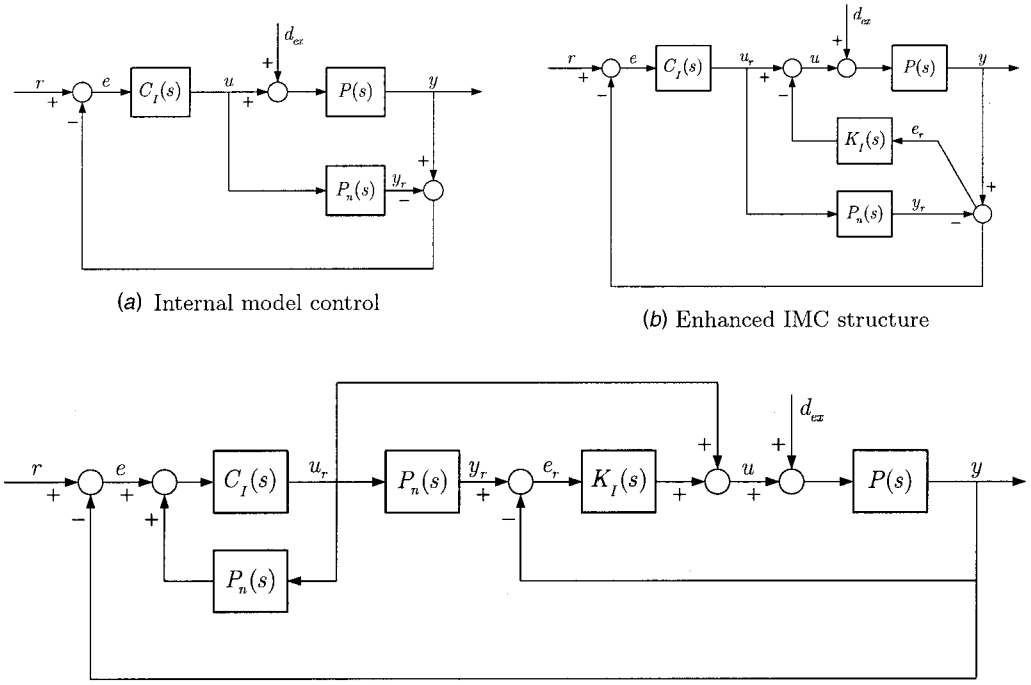

(a) Internal model control

(b) Enhanced IMC structure

(c) Enhanced IMC structure in the RIC framework

Fig. 10 Enhanced IMC and its equivalent structure in the RIC framework

as Eq. (20) or (26), the performance of RCA and DOB as well as RIC are exactly the same as will be shown in the simulation.

3.3 Enhanced IMC in the RIC Framework. Based on the conventional structure of IMC system shown in Fig. 10(*a*), a novel IMC with enhanced robustness was developed by Zhu et al. [13]. This scheme is shown in Fig. 10(*b*), and it is called the enhanced IMC. It is obvious that based on the conventional IMC structure, an additional path is appended to the original system within the plant-model parallel structure, where $C_I(s)$ is an IMC controller and $K_I(s)$ is a complementary IMC compensator. By inserting this additional path into the original IMC system, a complementary control input generated from the plant-model error is injected into the output of the original IMC controller. Hence it can be seen that the additional IMC compensator $K_I(s)$ can further reduce the effects of possible uncertainties and external disturbances, compared with the conventional IMC system.

As can be seen from the above discussion, the function of the additional IMC compensator is to make the plant more insensitive and robust to system uncertainties as well as external disturbance. Since $K_I(s)$ does not have a close relationship with $C_I(s)$, it can be analyzed independently from $C_I(s)$. Reconstructing the enhanced IMC system, we can obtain an equivalent structure of the enhanced IMC system whose structure is shown in Fig. 10(*c*). The internal-loop part without $C_I(s)$ has an equivalent structure with RIC and external-loop controller $C(s)$ can be expressed as

$$C(s)=\frac{C_I(s)}{1-P_n(s)C_I(s)} \quad \text{or} \quad C_I(s)=\frac{C(s)}{1+P_n(s)C(s)}. \tag{28}$$

As a result, it can be seen that the enhanced IMC can be restructured to the RIC based controller with the relations of Eq. (28).

4 Design of Disturbance Compensation Method

In the previous section, it is shown that there are inherent equivalences between DOB, RCA, and enhanced IMC. Among them, since DOB is the most popular method, DOB design in the RIC framework is discussed in this section.

Consider a high-speed/high-accuracy positioning system as one of the specific applications. Since the equation of motion is given by Eq. (13), the following second order model $P_n(s)$ can be chosen:

$$P_n(s)=\frac{1}{J_n s^2+B_n s}. \tag{29}$$

If $K(s)$ is designed as a PD controller:

$$K(s)=K_p+K_d s \tag{30}$$

where $K_p=gB_n$ and $K_d=gJ_n$, then the following Q-filter of DOB is obtained from Eq. (12):

$$Q(s)=\frac{g}{s+g}, \tag{31}$$

which is the first-order filter suggested by Ohnishi [20]. It is notable that if $P_n(s)$ is chosen as a double integrator plant, that is, $B_n=0$, then a derivative controller can be obtained to achieve the same $Q(s)$ in Eq. (31).

More specially, consider the case that the task is to achieve about ϕ rad phase lead effect at specified frequency with PI controller. Thus, $K(s)$ should be designed as a lead compensator with PI controller:

$$K(s)=K_L\left(\frac{Ts+1}{\alpha Ts+1}\right)\left(1+\frac{1}{T_I s}\right), \tag{32}$$

where $T_I=J_n/B_n$ and α is given by

$$\alpha=\frac{1-\sin(\phi)}{1+\sin(\phi)}. \tag{33}$$

From Eq. (12), therefore $Q(s)$ has the form of

$$Q(s)=\frac{Ts+1}{\left(\frac{J_n\alpha T}{K_L}\right)s^3+\left(\frac{J_n}{K_L}\right)s^2+Ts+1} \tag{34}$$

and the frequency where the phase is maximum is given by

$$\omega_{\max}=\frac{1}{T\sqrt{\alpha}}. \tag{35}$$

If $K_L=J_n/(3\tau^2)$, $T=3\tau$, and $\alpha=1/9$ are substituted into Eq. (34), then $Q(s)$ is expressed as

$$Q(s)=\frac{3(\tau s)+1}{(\tau s)^3+3(\tau s)^2+3(\tau s)+1}, \tag{36}$$

which is well known Q_{31}-filter [3,7,8,10,11,23,24]. This analysis gives very important meaning to the design of Q-filter in DOB. It is notable to see that the maximum phase contribution of the lead compensator in Eq. (32) is obtained as

$$\phi_{\max}=\sin^{-1}\left(\frac{1-\alpha}{1+\alpha}\right)\approx 53 \text{ deg} \tag{37}$$

and the frequency where the phase is maximum is given by

$$\omega_{\max}=\frac{1}{\tau}. \tag{38}$$

The PI controller part in Eq. (32) reduces the steady-state error at the cost of a phase decrease below the break point at $\omega=B_n/J_n$. Therefore, B_n/J_n should be located at a frequency substantially less than the crossover frequency so that the system's phase margin is not affected very much. This quantitative analysis and design was difficult in the previous typical DOB design. This analysis implies that the proposed unified framework can provide a systematic insight in the design of $Q(s)$. Instead of selecting $Q(s)$, we can design $Q(s)$ from the nominal model $P_n(s)$ and desired $K(s)$ which can produce desired specification. This is the basic difference in the design of $Q(s)$ from other previous methods.

Note also that these analyses were obtained for the unity feedback system in Fig. 5. By using Eq. (12), it can be shown that the structure of DOB is also equivalently changed to the structure of RIC in Fig. 2 with a nominal model $P_n(s)$. Thus, $F(s)$ in Eq. (12) is approximated to PD type controller if we use Eq. (31) or (34) and this leads the phase of the closed-loop system. Therefore, in order to design DOB with optimal sense, the characteristics of the unity feedback system and prefilter $F(s)$ should be considered at the same time.

5 Simulation

5.1 Comparative Simulation. The RIC, DOB, RCA, and enhanced IMC control systems are simulated in MATLAB environment. Let the real plant with uncertainty be expressed as

$$P(s)=\frac{1}{Js^2+Bs}=\frac{1}{(J_n+\Delta_J)s^2+(B_n+\Delta_B)s} \tag{39}$$

where $J_n=0.3$ V/(m/s^2) and $B_n=0.15$ V/(m/s) are the nominal value of J and B, and Δ_J and Δ_B are their estimation errors. Thus, the nominal model $P_n(s)$ is given by

$$P_n(s)=\frac{1}{J_n s^2+B_n s} \tag{40}$$

and, from Eq. (3), the multiplicative uncertainty can be obtained as

$$\Delta_M(s)=-\frac{\Delta_J s+\Delta_B}{(J_n+\Delta_J)s+(B_n+\Delta_B)}. \tag{41}$$

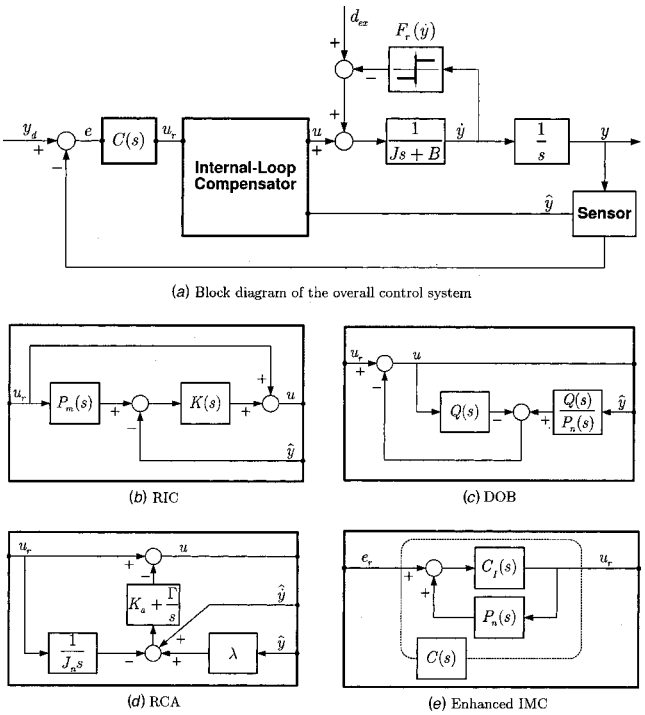

Fig. 11 Overall control system and internal-loop compensators

If the parameter uncertainties are given by $\Delta_J=-0.1$ V/(m/s^2) and $\Delta_B=-0.05$ V/(m/s), then $|\Delta_M(j\omega)|$ is 0.5 for all ω. Stiction and Coulomb friction are also added to the plant, whose magnitudes are 0.2 V and 0.1 V, respectively. The units [V/(m/s^2)], [V/(m/s)], [V] are due to the assumption that the equation of motion is obtained from the relation between the voltage output [V] and real displacement [m] of the plant. Figure 11 shows the overall control structure with internal-loop compensator and feedback controller. The feedback controller $C(s)$ is chosen as PD controller:

$$C(s)=K_p+K_d s \tag{42}$$

where K_p is 5000 and K_d is 300. The feedback signal used in internal-loop compensator is the position signal measured through the sensor that has 2 μm resolution. The velocity is estimated by the backward differentiation of position signal. The fifth order polynomial function is used to specify the position, velocity, and acceleration at the beginning and end of path:

$$y_d=y_t\left[6\left(\frac{t}{T_r}\right)^5-15\left(\frac{t}{T_r}\right)^4+10\left(\frac{t}{T_r}\right)^3\right] \tag{43}$$

where y_t is the target position given by 30 mm and T_r is the rising time given by 0.5 s. Control sampling frequency is 1000 Hz and all controllers are discretized by using the bilinear transformation.

In Fig. 11(b), the reference model is chosen as the same as the nominal model of Eq. (40) and the compensator $K(s)$ is chosen as PD control:

$$P_m(s)=P_n(s), \quad K(s)=(gB_n)+(gJ_n)s \tag{44}$$

where g is 100. By using Eq. (12), the $Q(s)$ of DOB used in Fig. 11(c) is calculated as

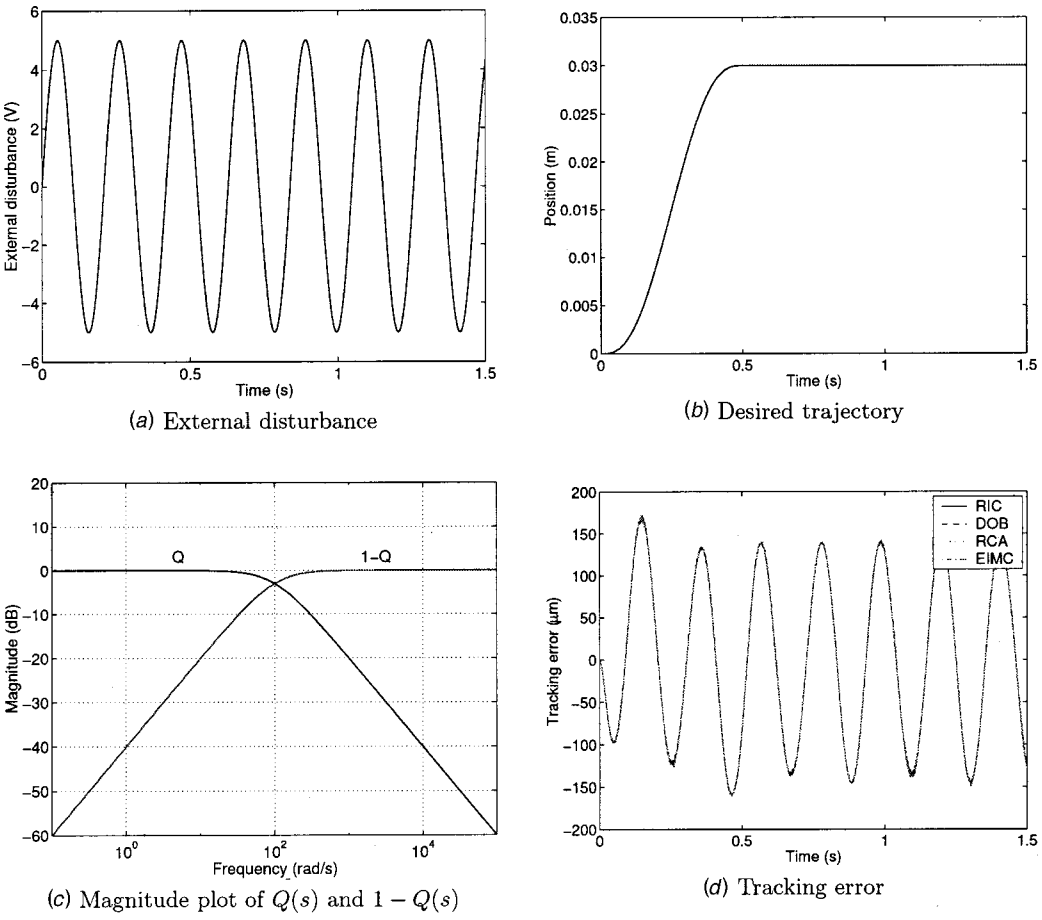

(*a*) External disturbance

(*b*) Desired trajectory

(*c*) Magnitude plot of $Q(s)$ and $1-Q(s)$

(*d*) Tracking error

Fig. 12 Simulation results of RIC, DOB, RCA, and enhanced IMC

$$Q(s)=\frac{g}{s+g} \tag{45}$$

to provide same control environment. The above selections of RIC and DOB are shown in Eq. (30), (31) and will make the whole control systems have same characteristics. If the Γ and K_a of RCA in Fig. 11(*d*) are selected so that

$$\Gamma=0, \quad K_a=gJ_n, \tag{46}$$

then, from Eq. (26), the characteristics of RCA become the same too. And also, in Fig. 11(*e*), if the enhanced IMC compensator $K_I(s)$ is chosen as same as $K(s)$ of RIC and $C_I(s)$ is chosen as

$$C_I(s)=\left[\frac{J_ns^2+B_ns}{J_ns^2+(B_n+K_d)s+K_p}\right](K_p+K_ds), \tag{47}$$

then, from Eq. (28), the characteristics of the whole closed-loop system with RIC, DOB, RCA, and enhanced IMC become the same.

To compare and verify the simulation results of these methods, the external disturbance signal shown in Fig. 12(*a*) is added to control input, where the signal is a 30 rad/s sinusoid. Figure 12(*b*) shows the desired trajectory. Figures 12(*c*) and (*d*), respectively, show the magnitude plot of $Q(s)$ and $1-Q(s)$ in frequency domain, and tracking errors when the four internal-loop compensators are applied to the system of Fig. 11(*a*). As can be seen here, the results show the equivalent characteristics of RIC, DOB, RCA, and enhanced IMC.

Of course, the other parameters such as more optimized $Q(s)$ of DOB, and K_a, Γ of RCA can be selected to further improvement of performance and disturbance attenuation. But the point is that it can be always shown that there is an equivalence between them through RIC framework such as Eq. (12), (26), and (28). Therefore, a simple comparison of DOB, RCA, and enhanced IMC in frequency domain and/or time domain has no crucial meaning, rather it is more important whether the controller has a structure to be designed optimally for a given system.

5.2 $Q(s)$ Design. In order to show that the proposed RIC structure gives a general design framework for the model based disturbance compensating methods, a simple design example is shown in this section. As discussed before, since DOB is the most popular method, DOB design in the RIC framework is discussed.

Now, let the task be to achieve about 30 deg phase lead effect at specified frequency with PI controller in the DOB closed-loop. Thus, the lead compensator proposed in Eq. (32) should be used. From Eq. (33), α is obtained as 1/3 and if $K_L=J_n/(3\tau^2)$ and $T=3\tau$, then $Q(s)$ is obtained by

$$Q(s)=\frac{3(\tau s)+1}{3(\tau s)^3+3(\tau s)^2+3(\tau s)+1} \tag{48}$$

and the frequency where the phase is maximum is given by

$$\omega_{\max}=\frac{1}{\sqrt{3}\tau}. \tag{49}$$

If $\omega_{\max}$ is set to 65 rad/s, then bode magnitude plots of $Q(s)$, $1-Q(s)$, and the tracking error when the DOB with this $Q(s)$ is applied to the system of Fig. 11(*a*) are obtained as shown in Fig. 13. The results for $Q_{31}(s)$ of Eq. (36) which has the same cutoff frequency as $Q(s)$ in Eq. (48) are also shown in this figure. It is notable that the characteristics of $1-Q(s)$ and $1-Q_{31}(s)$ are

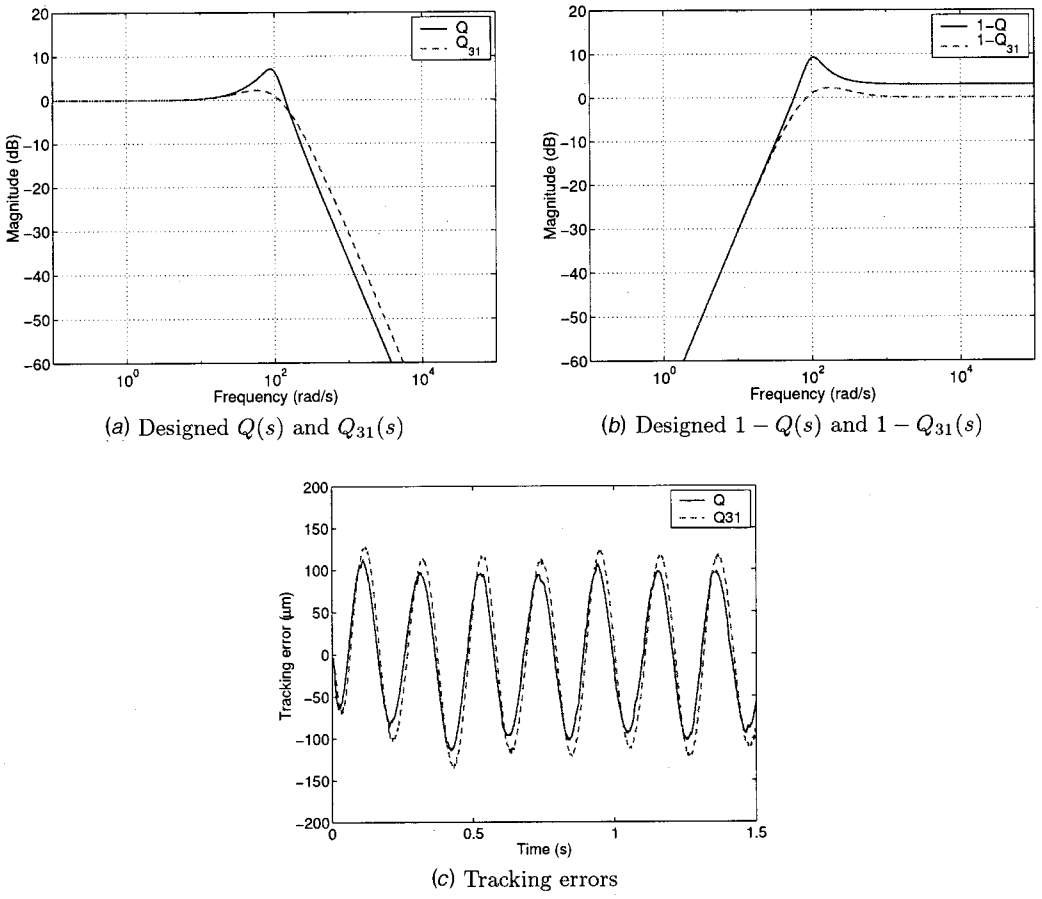

(a) Designed $Q(s)$ and $Q_{31}(s)$

(b) Designed $1-Q(s)$ and $1-Q_{31}(s)$

(c) Tracking errors

Fig. 13 Bode magnitude plots of designed $Q(s)$, $Q_{31}(s)$ and tracking error

nearly the same in the low frequency range. In Fig. 13(c), the tracking error of the newly designed $Q(s)$ shows better performance than that of $Q_{31}(s)$. Through these results, it can be easily seen that Q-filter of DOB can be systematically designed based on the reference model and the designed compensator in the RIC framework. On the other hand, it was very difficult to design $Q(s)$ itself to meet the above given task in the typical DOB design framework.

In a similar manner, many kinds of control methods based on feedback error can be used to design the compensator $K(s)$ and the low-pass filter $Q(s)$ for perturbed $P_n(s)$, such as LQ, $\mathcal{H}_2$, and $\mathcal{H}_\infty$ control.

6 Conclusion

In a unified framework, an analysis and design method of robust motion controllers with two-loop structure was proposed. Since the proposed RIC has a general structure, robust controllers with two-loop can be analyzed in the RIC framework and structural relationships can be addressed. It was shown that there are inherent equivalences between RIC, DOB, RCA, and enhanced IMC, and the proposed RIC structure can give general design framework for these algorithms. Through these equivalent characteristics, design of robust controllers can be done systematically. The equivalent characteristics of these internal-loop compensators and the validity of the proposed design method were verified by simulation.

References

[1] Nakao, M., Ohnishi, K., and Miyachi, K., 1987, "A Robust decentralized joint control based on interference estimation," *Proc. 1987 IEEE Int. Conf. on Robotics and Automation*, pp. 326–331.

[2] Umeno, T., and Hori, Y., 1991, "Robust speed control of dc servomotors using modern two degrees-of-freedom controller design," IEEE Trans. Ind. Electron., **38**(5), pp. 363–368.

[3] Lee, H. S., and Tomizuka, M., 1996, "Robust motion controller design for high-accuracy positioning systems," IEEE Trans. Ind. Electron., **43**(1), pp. 48–55.

[4] Ohnishi, K., Shibata, M., and Murakami, T., 1996, "Motion control for advanced mechatronics," Mechatronics, **1**(1), pp. 56–67.

[5] Iwasaki, M., Shibata, T., and Matsui, N., 1999, "Disturbance-observer-based nonlinear friction compensation in table drive system," Mechatronics, **4**(1), pp. 3–8.

[6] Bickel, R., and Tomizuka, M., 1999, "Passivitiy-based versus disturbance observer based robot control:equivalent and stability," ASME J. Dyn. Syst., Meas., Control, **121**, pp. 41–47.

[7] Kempf, C. J., and Kobayashi, S., 1999, "Disturbance observer and feedforward design for a high-speed direct-drive positioning table," IEEE Trans. Control Syst. Technol., **7**(5), pp. 513–526.

[8] Tesfaye, A., Lee, H. S., and Tomizuka, M., 2000, "A sensitivity optimization approach to design of a disturbance observer in digital motion control systems," Mechatronics, **5**(1), pp. 32–38.

[9] Choi, H.-T., Kim, B. K., Suh, I. H., and Chung, W. K., 2000, "Design of robust high-speed motion controller for a plant with actuator saturation," ASME J. Dyn. Syst., Meas., Control, **122**(3), pp. 535–541.

[10] Yao, B., Al-Majed, M., and Tomizuka, M., 1997, "High performance robust motion control of machine tools: An adaptive robust control approach and comparative experiments," Mechatronics **2**(2), pp. 63–76.

[11] Yi, L., and Tomizuka, M., 1999, "Two-degree-of-freedom control with robust feedback control for hard disk servo systems," Mechatronics **4**(1), pp. 17–24.

[12] Choi, B.-K., Choi, C.-H., and Im, H., 1999, "Model-based disturbance attenuation for CNC machining centers in cutting process," Mechatronics **4**(2), pp. 157–168.

[13] Zhu, H. A., Hong, G. S., Teo, C. L., and Poo, A. N., 1995, "Internal model control with enhanced robustness," Int. J. Syst. Sci., **26**(2), pp. 277–293.

[14] Kim, B. K., and Chung, W. K. 2001, "Unified analysis and design of robust disturbance attenuation algorithms using inherent structural equivalence," *Proc. 2001 American Control Conference*, pp. 4046–4051.

[15] Kim, B. K., and Chung, W. K., 2001, "Performance tuning of sliding mode controllers: Structural analysis approach," *Proc. 2001 American Control Conference*, pp. 1513–1518.

[16] Khalil, H. K., 1992, *Nonlinear Systems*, Macmillan, NY.

[17] Kim, B. K., and Chung W. K., 2001, "Performance predictable design of

robust motion controllers for high-precision servo systems,'' *Proc. 2001 American Control Conference*, pp. 2249–2254.
[18] Kim, B. K., Choi, H. T., Chung, W. K., Suh, I. H., Lee, H. S., and Chang, Y. H., 1999, ''Robust time optimal controller design for HDD,'' IEEE Trans. Magn., **35**(5), pp. 3598–3600.
[19] Kim, B. K., Chung, W. K., Choi, H. T., Suh, I. H., and Chang, Y. H., 1999, ''Robust optimal internal loop compensator design for motion control of precision linear motor,'' *Proc. 1999 IEEE Int. Symposium on Industrial Electronics*, pp. 1045–1050.
[20] Ohnishi, K., 1987, ''A new servo method in mechatronics,'' Trans. Japanese Society of Electrical Engineering, **107-D**, pp. 83–86.
[21] Umeno, T., Kaneko, T., and Hori, Y., 1993, ''Robust servosystem design with two degrees of freedom and its application to novel motion control of robot manipulators,'' IEEE Trans. Ind. Electron., **40**(5), pp. 473–485.
[22] Yamada, K., Komada, S., Ishida, M., and Hori, T., 1997, ''Analysis and classical control design of servo system using high order disturbance observer,'' *Proc. 1997 IEEE Int. Conf. on Industrial Electronics, Control, and Instrumentation*, pp. 4–9.
[23] Tomizuka, M., 1994, ''Controller structure for robust high-speed/high-accuracy digital motion control,'' *Tutorial of 1994 IEEE Int. Conf. on Robotics and Automation*.
[24] Oh, Y., and Chung, W. K., 1999, ''Disturbance-observer-based motion control of redundant manipulators using inertially decoupled dynamics,'' Mechatronics, **4**(2), pp. 133–146.

Transient Improvement of Variable Structure Controlled Systems Via Multi-Model Switching Control

Maria Letizia Corradini
Dipartimento di Ingegneria dell'Innovazione, Università di Lecce, via Monteroni, 73100 Lecce, Italy
e-mail: letizia.corradini@unile.it

Giuseppe Orlando
Dipartimento di Elettronica e Automatica, Università di Ancona, via Brecce Bianche, 60131 Ancona, Italy
e-mail: orlando@ee.unian.it

A solution is presented in this note to the problem of improving the transient response of a MIMO nonlinear system driven by a VSC law, in the presence of large plant uncertainties. The proposed control scheme is given in terms of a supervisor and of a deterministic time-varying compensator, built using sliding-mode control and assuming a finite number of possible different configurations. The task of the supervisor is that of guiding the scanning among the elements of the family, according to a suitably defined experimental test. The proposed approach noticeably improves the performances of sliding-mode control in the presence of large plant uncertainties, and has the substantial advantage of a great simplicity of design and implementation. Moreover, even in case of a large number of configurations constituting the stabilizing family, it has been shown to be able to attain the stabilizing controller in an arbitrarily small time interval. Another appealing feature of the paper consists in the inclusion of an intelligent adaptation scheme in the control algorithm.
[DOI: 10.1115/1.1470172]

1 Introduction

The problem of designing a controller able to stabilize a closed-loop system despite possible variations of a set of physical parameters within a prescribed range can be said to be a basic issue crossing the whole control theory literature. In particular, great advances have been achieved, in recent years, in the research on robust nonlinear feedback control, especially under the hypothesis of full state availability (see [1–5]). In this framework, Sliding Mode (SM) control [6] undoubtedly received great attention for its well known robustness feature, in spite of matched disturbances and/or bounded parameter uncertainties. Under suitable conditions, in fact, ''the sliding -mode of a Variable Structure Control (VSC) system is invariant, more than just robust, with respect to system perturbations and external disturbances'' [7]. Nevertheless, the high-speed character of VSC, i.e., the occurrence of the well known chattering phenomenon, restricts the practical implementation of such controllers. The physical bounds on control effort, in fact, limit the bandwidth of the closed-loop system and, if the response speed is excessive, sliding mode may fail, leading to poor transient responses or even instability. It follows that the presence of large plant uncertainties cannot be easily dealt with in practice, since the resulting excessive magnitude of discontinuous control severely affects the closed loop performances. Nevertheless, practical control systems design has often to comply with uncertain parameters varying in a wide range [8].

To face this problem, a number of adaptation mechanisms have been proposed in the literature, using also neural nets and fuzzy logic [9–11]. A remarkable research line, within this context, is the so called adaptive sliding mode control area, which originated from the combination, for some classes of nonlinear systems, of control strategies commonly referred to as adaptive control techniques with VSC [12–15]. Adaptive controllers, in fact, can ensure indeed global regulation and tracking properties, but usually require a backstepping design approach which is often very involved even for low dimension plants. To enhance robustness and reduce the computational load, control strategies belonging to this area have been recently coupled with sliding mode control. The addressed class of systems typically includes feedback linearizable systems that can be transformed into parametric pure and strict feedback form systems [13–15]. In some cases, constant and/or polynomial type bounds in the states are supposed to be present [16,17].

Independently on how a suitable sliding surface is designed, and under the hypotheses of bounded uncertainties, a solution is presented in this note to the problem of improving the transient response of a MIMO nonlinear system driven by a VSC law. It has the substantial advantage of a great simplicity of design and implementation, if compared to adaptive/VSC algorithm and neural nets based adaptation mechanisms. The proposed scheme is based on switching control, which is a rapidly emerging area mainly investigated, in the past decade, in the framework of linear adaptive control systems [18–23]. Although a number of interesting results have been presented for linear control systems [24–27], very few literature reports about switching control for nonlinear systems, at least at the authors' knowledge, are available.

The control scheme proposed here is constituted by a nonlinear, time-varying controller whose time adaptation is governed by a suitably defined event driven switching scheme. The controller consists of: (i) a nonlinear, time-varying controller which assumes a finite number of different possible configurations, among which there is at least one stabilizing the plant; (ii) the definition of a suitable transition function guiding the switching among the elements of the family; (iii) the experimental identification of the controller actually stabilizing the system.

A further improvement consists in the inclusion of an intelligent adaptation scheme in the control algorithm. The idea is that of defining a suitable performance index, and to switch the time-varying controller to the configuration producing the minimum index at each time instant. The convergence of the algorithm has been proved. This paper extends results previously obtained [28,29].

Contributed by the Dynamic Systems and Control Division of THE AMERICAN SOCIETY OF MECHANICAL ENGINEERS. Manuscript received by the Dynamic Systems and Control Division July 7, 2000. Associate Editor: Y. Chait.